The importance of water velocity on nitrate removal in vegetated waterways

Giuseppe Castaldelli, Vassilis Aschonitis, Fabio Vincenzi, Elisa Anna Fano, Elisa Soana*

Department of Life Sciences and Biotechnology, University of Ferrara, Via L. Borsari 46 - 44121 Ferrara – Italy
*Corresponding author: elisa.soana@unife.it

Abstract

The extended networks of drainage and irrigation canals in agricultural landscapes can provide extremely important ecosystem services related to nutrient removal from flowing water. The nutrient mitigation capacity depends on several biotic and abiotic factors, among which flow velocity is poorly explored and generally omitted from the parameterization of nutrient removal processes in these environments. The present work reports new insights on the role of flow velocity in regulating N removal via denitrification in vegetated sediments colonized by *Phragmites australis* (Cav. Trin. ex Steud). Undisturbed sediments with plants and bare sediments were sampled from a drainage canal of a lowland sub-basin of the Po River (northern Italy) in order to create outdoor experimental mesocosms. Denitrification was investigated in these mesocosms for four flow velocities 0, 1.5, 3 and 6 cm s^{-1}, by simultaneous measurements of NO_3^- consumption and N_2 production based on analyses of N_2:Ar by Membrane Inlet Mass Spectrometry. Vegetated sediments were found more efficient in converting NO_3^- to N_2 via microbial-mediated denitrification (27-233 mmol N m^{-2} d^{-1}) than bare sediments (18-33 mmol N m^{-2} d^{-1}). Flow velocity had a significant impact on N metabolism in sediments colonised by emergent vegetation exhibiting one order of magnitude raise in NO_3^- removal and denitrification rates when flow velocity increased from 0 to 6 cm s^{-1}. The results highlighted that the increase of flow velocity in slow-flow vegetated shallow waterways, can enhance the rate of NO_3^- supply through the diffusive boundary layer, promoting N removal by denitrification. The importance of vegetation is related to the fact that provides multiple interfaces (e.g. rhizosphere and epiphytic biofilms) that promote the development and activity of bacterial communities responsible for N dissipation. This study highlights the importance of flow velocity as a key factor for the development of best management practices aiming at maximizing depuration potential through denitrification in slow-flow waterways.

Keywords

NO_3^- removal, aquatic vegetation, water velocity, canal network, denitrification, N_2 open-channel method

Author contributions: GC, VA, EAF and ES conceived and designed the experiments and wrote the paper; FV performed the experiments and the laboratory analyses; ES and VA analyzed the data.

1. Introduction

Nitrogen (N) pollution and eutrophication are unsolved issues and their contribution on habitat deterioration, biodiversity loss and climate change are more and more severe worldwide (Leip et al., 2015). At the same time the simplification of aquatic habitats is continuing with a further loss of watershed capacity to buffer excessive N loads (Valiela and Bowen, 2002; Kareiva et al., 2007). In industrialized countries, some actions to invert this trend have been encouraged by the enactment of policies for water protection, as the Clear Water Act in the United States and the Water Framework Directive in the European Union, but the results remain modest or, according to some researchers, null (Weigelhofer et al., 2013; Garnier et al., 2014; Arheimer and Pers, 2016). Budget simulations in lowland agricultural watersheds have highlighted that wetland contribution in removing the N surplus is at present minimal (Verhoeven et al., 2006; Bartoli et al., 2012). Aquatic environments such as wetlands and rivers have been restored in the context of reclamation initiatives but at inferior level of environmental quality compared to the one present before the industrial development of agriculture and likely not sufficient to mitigate the current N loads. However, agricultural landscapes maintain the capacity to dissipate part of this N excess, i.e. converting it from reactive forms to gaseous inert N_2, thanks to the buffer potential exerted by the extended networks of drainage and irrigation ditches and higher order canals (Törnqvist et al., 2015; Romero et al., 2016). This function can be ascribed to some attributes of water medium that promote N processing and removal, such as long water residence time, high hydrodynamic energy favouring water column recirculation, elevated primary production, organic matter availability, hypoxic conditions on the bottom, and the presence of multiple interfaces that favour differentiated microniches and a rich microbial community (Revsbech et al., 2005; Veraart et al., 2016). Nevertheless, their role as providers of ecosystem services, e.g. as N metabolic regulators, is generally not considered in the current management practices (Dollinger et al., 2015; Biggs et al., 2017).

Due to differences in landscape position (e.g. proximity to N sources), functions and management, ditches and canals may be extremely heterogeneous in term of hydraulic parameters (e.g. flow, velocity, water level fluctuations), water quality, benthic compartment (e.g. quality and quantity of organic matter, texture), and biological communities. The regulation of N retention and removal in small watercourses has been explored in relation to abiotic (e.g. inorganic N concentration, organic loading, redox conditions) and biotic controlling factors (e.g. communities of primary producers), and their multiple interactions (Pierobon et al., 2013; Taylor et al., 2015; Veraart et al., 2016). The mitigation potential of vegetated canals towards N has been less extensively studied compared to wetlands (Ilyas and Masih, 2017), and in the majority of cases, it is limited to a black-box approach, such as in-out mass balance of dissolved nitrogen species, which does not allow validating the direct hypothesis of nitrate (NO_3^-) removal by denitrification (e.g., Xiong et al., 2015; Moore et al., 2016). The relative contribution of denitrification has been poorly investigated, especially when assessed as direct measurement of its end-product, i.e. N_2 (Kröger et al., 2014; Taylor et al., 2015; Castaldelli et al., 2015; Soana et al., 2017).

In ditches and canals of intensively cultivated basins, NO_3^- is generally not limited and water velocity may be a regulatory factor of diffusive boundary layers and thus of NO_3^- availability, especially in zones of rapid consumption, such as in the rhizosphere and epiphytic biofilms. Nonetheless, water velocity as a key driver controlling N removal remains poorly if not at all explored. Ecosystem-level metabolism is strongly affected by the solute mass transfer from the water column to the bioactive surfaces through the diffusive boundary layer, which usually acts as a limiting agent for nutrient and gas exchange (Silvester and Sleigh, 1985; Larned et al., 2004). Increasing velocities decrease the thickness of the boundary layer adjacent to uptake surfaces resulting in shorter diffusive distances, thus enhancing solute mass transfer and stimulating metabolic processes (Madsen and Sand-Jensen, 1991; Eriksson, 2001; Arnon et al., 2013). NO_3^- losses by denitrification in watercourses is governed by its supply from the water column to anoxic sediments or other interfaces where denitrification occurs (i.e. epiphytic biofilms on submersed

100 vegetation). In the case of NO_3^- diffusion in sediments, the most important process of NO_3^- supply
101 to denitrifiers is usually the convective transfer, which depends on water velocity and the presence
102 of aquatic vegetation that increases turbulent flow and water column mixing (Silvester and Sleigh,
103 1985; Nikora, 2010). Increasing velocities simultaneously promote more oxic conditions in the
104 superficial sediment, thus stimulating aerobic metabolism and inhibiting denitrification (Arnon et
105 al., 2007a), or forcing denitrification zone deeper into the sediments (O'Connor and Hondzo, 2007).
106 The effects of flow velocity on biogeochemical dynamics has been investigated in benthic
107 biofilms (e.g., Madsen and Sand-Jensen, 1991; Larned et al., 2004; Arnon et al., 2013) and in
108 biofilms growing on aquatic vegetation (Eriksson and Weisner, 1999; Eriksson, 2001), focusing
109 mainly on photosynthesis, respiration and macronutrient assimilation. With respect to N cycling,
110 fewer investigations have been performed on the relationship between flow conditions and NO_3^-
111 removal in laboratory cultivated periphyton mats (Eriksson, 2001; Arnon et al., 2007a,b; Carleton
112 and Mohamoud, 2013), but no measurements of NO_3^- consumption and N_2 production were
113 performed simultaneously. Thus, this important issue still remains poorly explored and to our
114 knowledge, no studies have previously investigated the effects of water flow velocity on N removal
115 via denitrification in intact sediments colonized by emergent vegetation with naturally developed
116 epiphytic communities.
117 This paper reports new insights on the role of flow velocity in regulating nitrogen removal via
118 denitrification in presence of a monospecific stand of *Phragmites australis* (Cav. Trin. ex Steud).
119 Experiments were performed using mesocosms representative of field conditions previously
120 described in studies of N removal in vegetated canals fed by NO_3^- -rich water (Pierobon et al., 2013;
121 Castaldelli et al., 2015). N removal was quantified by the simultaneous measurement of NO_3^-
122 consumption and N_2 production (N_2 open-channel method). Three velocities (1.5, 3, and 6 cm s^{-1})
123 along with a stagnant control condition were set to cover the typical range of variation in drainage
124 canals and ditches in lowland agricultural basins.

By working in field conditions, it is extremely difficult if not impossible, to isolate the effect of one parameter, such as water velocity, on denitrification, since other important parameters, e.g. nitrate availability and temperature, may vary at the same time. For instance, in shallow waterways, water temperature increases rapidly in summer daylight, affecting gas solubility and the exchange with the atmosphere and making difficult the application of the N_2 open-channel method (Reisinger et al., 2016). To overcome this limitation, mesocosm simulations allow the standardization of the experimental conditions and the systematic manipulation of a single or a limited suite of variables. Moreover, they represent a good compromise between the application of controlled conditions, typical of the laboratory approach, and the realism of field measurements that aims at the scaling-up of the results.

The present experiments were used to test the hypothesis that flow velocity is a fundamental physical property that regulates denitrification. The results of the study aim to highlight the importance of flow velocity, since it is usually omitted in the parameterization of the N depuration capacity of waterways.

2. Material and Methods

2.1 Mesocosm construction

Mesocosms were built using water and undisturbed sediment-plants samples in order to represent the conditions of vegetated drainage ditches and canals of the lower Po plain (Northern Italy). The samples were taken by a drainage canal of Ferrara Province (44°48'53.17"N; 11°43'23.14"E) where denitrification and NO_3^- removal rates were previously measured by means of the N_2 open-channel and N mass balance methods (Castaldelli et al., 2015).

Mesocosms (Fig. 1a) were designed to simulate vegetated waterways or wetlands with moving water. The chambers were built as follows: an external tube with internal diameter of 29 cm and an internal tube with external diameter of 12 cm were positioned concentrically on a plexiglass circular base, to define an annulus of total surface 547 cm^2 (annular radius width 8.5 cm, internal

151 height 65 cm). Mesocosm height was set to respect the original features of the sampled canal, which
152 was described by 25 cm of sediment including rhizosphere and 35 cm of water column.

153 Sediment colonised by a dense stand of *P. australis* (1300-2200 gDW m^{-2}) and bare sediment
154 of nearby positions were sampled using a steel shovel having a blade with finely sharpen edge.
155 Parcels of sampled sediment were placed in the annular plexiglass chambers to define a continuous
156 annulus of sediment. Three chambers with sediment and *P. australis* (18-30 plants in each
157 mesocosm) and three chambers only with sediment were developed and they were transferred from
158 the field to an outdoor, non-shaded area at the Department of Life Sciences and Biotechnology,
159 University of Ferrara, and maintained under natural weather conditions.

160 The choice of the previously described annular chamber mesocosms was made for the
161 following reasons:

162 • mesocosms are more stable environments compared to open systems and can provide more
163 robust replications for testing one variable (e.g. flow velocity, which cannot be regulated in
164 the field) keeping controlled other important variables such as NO_3^- concentration and
165 temperature;
166 • the proposed dimensions of mesocosms is compatible for determining a homogeneous flow
167 of water inside the whole annular chamber without sediment resuspension;
168 • the proposed dimensions of mesocosms allow an operatively viable hand collection of the
169 sediment by maintaining intact the rhizosphere without damaging the *P. australis* rhizomes.

170

171 *2.2 Pre-incubation procedure*

172 In an hour after sampling, chambers were brought to the laboratory and placed in two
173 separate cylindrical tanks (87 cm diameter and 105 cm high polyethylene containers) (Fig.1b), one
174 for vegetated replicates and one for replicates devoid of vegetation. Pre-incubation and incubation
175 procedures were performed according to standard protocols (Dalsgaard et al., 2000).

Water from the canal was used to fill gently the chambers and the tanks. Water mixing among the chambers of each tank end between the tanks was supported by aquarium pumps. The chambers were maintained submerged in canal water and they were allowed to equilibrate for one month before the incubations. Water level in the tanks was being controlled every day and water from the canal was added to compensate for evapotranspiration loss. Each tank was connected with a thermostat to maintain temperature constant at 26-27°C during pre-incubation and incubation procedures.

2.3 Incubation procedure

Each chamber was equipped with a 12 volts pump (Whale® submersible electric pump) connected to a multichannel electronic rheostat with a voltage regulation. Each pump was submerged at 4 cm below the water surface to prevent bubbling. A plastic tube connected to the pump was placed vertically in the water column and oriented in a way to create a flow within the chamber without sediment resuspension (Fig. 1a). Voltage level was regulated in each chamber to yield an average flow velocity of 0, 1.5, 3, and 6 cm s^{-1}, checked with a current meter, vertically and on the middle of the annular radius and in the middle of the water column.

Mesocosms incubations were performed both in dark (from 3:00 a.m. to 6:00 a.m.) and in light (from 10:30 a.m. to 01:30 p.m.) at each velocity to discriminate the effect of photosynthetic on N retention. A different velocity was applied each day in the mesocosms, from 0 to 6 cm s^{-1}. Incubations were repeated twice. The first experiment was performed in the middle of the summer (from 25.07.2016 to 28.07.2016) during four consecutive days of stable meteorological conditions, in order to minimize any unpredictable source of climatic variation. Average air temperature was 22.5±1.5°C and 28.7±2.4°C during dark and light incubations, respectively. Solar radiation during light phase averaged 670±190 W m^{-2} (University of Ferrara weather station). The second experiment was performed 25 days after (from 22.08.2016 to 25.08.2016). Solar radiation during

light phase was similar (730±100 W m^{-2}), but water temperature dropped of about 3°C (average air temperature 18.5±2.2°C and 26.0±1.9°C during dark and light incubations, respectively).

Before any incubation, the water in each of the two tanks was replaced with water sampled during the previous day from the canal, which was checked for NO_3^- and ammonium. Ammonium and nitrite concentrations were always below detection limits, suggesting that NO_3^- dominated N dynamics in the mesocosms. NO_3^- concentration was standardized to 100 µM at the zero time of each incubation by adding an appropriate volume of a stock NO_3^- solution (200 mM KNO_3). The value of 100 µM was chosen because it approximates the typical average NO_3^- availability in ditches and canals of the investigated area, which are mainly affected by non-point source pollution where ammonium and nitrite are constantly under the µM threshold (Pierobon et al., 2013; Castaldelli et al., 2015). Temperature and NO_3^- availability in water were maintained as similar as possible among incubations, and the only variables that were varied and that hence affected N removal process were water velocity and light conditions.

To initiate the determinations, the water level in the tanks was lowered below the chamber tops and zero-time water samples were collected. Water samples were withdrawn from the mid-depth of each mesocosm using a glass syringe, 5 times (from t0 to t4) at 45' interval over 3h to follow the temporal evolution of NO_3^- and N_2. At each sampling, water temperature, electrical conductivity and oxygen were also measured with a multiparametric probe. Samples for NO_3^- determinations were filtered through Whatman GF/F glass fiber filters, and transferred to polyethylene vials. NO_3^- was measured on a Technicon AutoAnalyser II (Armstrong et al., 1967; detection limit 0.4 µM; precision ±5%). Samples for N_2:Ar determinations were transferred into 12-ml gastight glass vials (Exetainer®, Labco, High Wycombe, UK), flushing at least 3 times the vial volume and preserved by adding 100 µl of 7M $ZnCl_2$ solution. The N_2:Ar ratio in water samples was measured within one week at the laboratory of Aquatic Ecology, University of Ferrara, by MIMS (Bay Instruments, USA; Kana et al., 1994), a PrismaPlus quadrupole mass spectrometer with an inline furnace operating at 600°C to allow for O_2 removal. The coefficient of variation calculated

from replicated N_2:Ar samples (n=10) was 10-fold lower (~0.04%) than N_2 measurements, similarly to Laursen and Seitzinger (2002). N_2 concentration was calculated from the measured N_2:Ar multiplied by the theoretical saturated Ar concentration at the sampling water temperature, which was determined from gas solubility tables (Weiss, 1970). N_2 production rates were calculated as described in the paragraph 2.4.

Additional samples for N_2O determinations were collected in the same way of those for N_2:Ar analysis. Dissolved nitrous oxide was measured by gas chromatography (Trace GC, 2000 Series, Thermo Finnigan, San Jose, CA, USA equipped with an ECD detector), but N_2O production was found negligible. N_2O production was also found negligible in field conditions as it was previously demonstrated by Castaldelli et el. (2015) after performing measurements in the same canal from which the samples were collected to build the chambers.

At the end of all incubations, density of *P. australis* stems, mean diameter of each stem, and mean height of submerged portion were measured in each vegetated mesocosm for the estimation of the total surface suitable for bacteria and microalgae biofilm. Daily plant N uptake was estimated from direct estimate of reed stand biomass, and the average relative growth rate for the summer period and the tissue N content, obtained from experimental campaigns previously performed in the same canal (Pierobon et al., 2013).

2.4 Calculation of NO_3^- removal and N_2 production rates

NO_3^- removal rate (mmol N m^{-2} h^{-1}) was calculated for each mesocosm from the rate of change in NO_3^- concentrations with time and expressed as per square meter. The water volume collected for analysis was overall <5% of the total volume included in each chamber while a correction factor was used to account for the loss of water volume from the five subsequent samplings.

The same set of equations given by Laursen and Seitzinger (2002) for open-channel denitrification were used at the mesocosm scale to model net N_2 fluxes. The general assumption is

253 that in an open-top mesocosm, where water flow is artificially set, N_2 concentrations evolve
254 temporally due to metabolic activity and as a function of temperature that affects the gas exchange
255 with the atmosphere, similarly to a Lagrangian transport in a natural watercourse (Laursen and
256 Seitzinger, 2002). The constant temperature conditions by thermostats in the tanks during
257 incubations maintained the stability of the gas fluxes across the water-atmosphere interface. This
258 approach determines net N_2 fluxes because the measured N_2 concentrations are the results of
259 production (i.e. denitrification including coupled nitrification/denitrification, anammox -Anaerobic
260 Ammonium Oxidation) and consumption (i.e. N fixation) processes. However, the terms
261 "denitrification" and "N_2 production" (or N_2 flux) are used interchangeably in the text, since the
262 contribution of anammox is usually low in eutrophic freshwater environments (Zhou et al., 2014;
263 Shen et al., 2016).

264 Net N_2 fluxes for each mesocosm were estimated at 1-min time steps using the following
265 input parameters in the equations of Laursen and Seitzinger (2002): measured N_2 and water
266 temperature at each sampling time, average flow velocity set in the mesocosm, dimension of the
267 moving parcel (water column height × annular radius), gas transfer velocity (k600), and Schmidt
268 number coefficient (−2/3 typical for water surfaces without waves, Jähne et al., 1987). The
269 reaeration coefficient of oxygen at 20°C (KO_2, 20°C, d^{-1}) was calculated from flow velocity *u* (m s^{-1})
270 and water depth *d* (m) by the general empirical equation by Genereux and Hemond (1992):

271 $$K_{O_2} = a \cdot \frac{u^b}{d^c}$$

272 The parameters of *a*, *b*, and *c* were obtained by the literature where measurements of gas transfer in
273 re-circulating cylindrical flumes were performed within velocity-depth ranges comparable to that
274 adopted in the present study (Isaacs and Gaudy, 1968; Eloubaldy, 1969; Isaac et al., 1969;
275 Negulescu and Rojanki, 1969; Padden and Gloyna, 1972). These equations have been tested and
276 applied in laminar flow channels, artificial flumes, and regular-shaped sewers (Cox, 2003) and often
277 identified as the most reliable choice in review studies about reaeration equations (Palumbo and

278 Brown, 2013). The transfer velocity of oxygen (kO_2, 20°C, cm h^{-1}) was obtained by multiplying the
279 reaeration coefficient by the average water column depth of each mesocosm, assuming a well-
280 mixed water column. The gas transfer velocity was finally normalized to a Schmidt number of 600
281 (k600, for CO_2 at 20 °C, cm h^{-1}) (Jähne et al., 1987; Wanninkhof, 1992). To quantify uncertainty,
282 the aforementioned set of equations given by Laursen and Seitzinger (2002) were applied varying
283 the gas transfer parameterizations and a range of N_2 production rates for each experimental
284 condition. The general equation of Genereux and Hemond (1992) for calculating the oxygen
285 reaeration coefficient cannot be used in stagnant waters. Moreover, when wind speed is almost null
286 as generally occurs in the lower Po valley, neither wind-based models are suitable (Cole and
287 Caraco, 1998). Under stagnant conditions, gas exchange is low but not null. Thus with a
288 conservative approach, we adopted the lower extreme of the k600 range obtained for 1.5 cm s^{-1}
289 velocity with the above reported depth-velocity equations.

290 The equations proposed by Laursen and Seitzinger (2002) for N_2 open-channel estimation
291 cannot be applied in stagnant conditions since a Lagrangian transport of the water parcel is required.
292 N_2 production rate (mmol N m^{-2} h^{-1}) was calculated for each mesocosm from the rate of change in
293 concentrations with time and expressed as per square meter, corrected for the N_2 efflux from the
294 water column to the atmosphere (Jacobs and Harrison, 2014), as N_2 concentrations were constantly
295 higher than the theoretical saturated N_2 concentration at the sampling water temperature. This
296 procedure assumes the N_2 concentrations in the mesocosm water column were at steady state. The
297 efflux was calculated as the product of the difference between the measured N_2 concentration in the
298 water column and the theoretical saturated N_2 concentration at the sampling water temperature
299 determined from gas solubility tables (Weiss, 1970), and the N_2 reaeration coefficient. The
300 estimates of KO_2 were converted to KN_2 based on the respective Schmidt numbers of this gas
301 calculated for water temperature at the sampling times, according to the polynomial fit given by
302 Wanninkhof (1992).

303 Hourly rates of NO_3^- removal and N_2 production were multiplied by the average number of
304 light and dark hours in the summer period of the investigated area (Allen et al., 1998) and summed
305 to obtain daily values (mmol N m^{-2} d^{-1}).
306
307 *2.5 Statistical analyses*
308 The effect of factors *velocity*, and *light condition* (light/dark) on NO_3^- removal and
309 denitrification in vegetated and bare mesocosms was tested by a two-way ANOVA. Statistical tests
310 were performed separately for data from bare and from vegetated mesocosms to exclude any
311 predictable significance due to plant activity. Previous studies have demonstrated that benthic N
312 dynamics are significantly affected by the presence of *P. australis* (Pierobon et al., 2013; Castaldelli
313 et al., 2015). Tuckey's post-hoc multiple comparison test was used to identify the significant
314 differences among velocity levels. Differences between NO_3^- removal and denitrification rates were
315 tested by Student's t-test. Normality (Shapiro–Wilk test) and homoscedasticity (Levene's test) were
316 previously examined. All datasets fulfilled the requirements for parametric tests. Statistical
317 significance was set at $p \leq 0.05$. Statistical analyses were performed with SigmaPlot 11.0 (Systat
318 Software, Inc., CA, USA). Average values are reported in graphs and tables with associated
319 standard deviation (std. dev.).
320
321 **3. Results**
322 *3.1 NO_3^- removal rates*
323 Initial mesocosm conditions were very similar among the incubations, as shown in Table 1.
324 For each velocity level, NO_3^- removal and denitrification rates were not statistically different
325 between the two sets of incubations ($p>0.05$), thus, results, tables and figures include pooled data.
326 During the 3-hour incubations, NO_3^- amounts in water of *P. australis* mesocosms decreased on
327 average by 61-88% and 82-90%, in dark and light conditions, respectively. NO_3^- depletion along
328 was also detected in bare sediment mesocosms and ranged between 5 and 13% considering both

329 dark and light conditions. NO_3^- removal rates were evaluated by monitoring the reduction over time
330 in water column concentrations. The reduction of NO_3^- versus time was linear in all cases indicating
331 that NO_3^- removal was not concentration dependent.

332 Across the velocity range, NO_3^- removal ranged between 1173±435 (stagnant condition, dark)
333 and 6543±803 µmol N m^{-2} h^{-1} (6 cm s^{-1}, light) in vegetated sediments, and between 520±236 (1.5
334 cm s^{-1}, light) and 1051±290 µmol N m^{-2} h^{-1} (3 cm s^{-1}, dark) in bare sediments (Fig. 2a). NO_3^-
335 removal rates were significantly different between light and dark conditions both in presence and
336 absence of *P. australis* (Table 2). For vegetated mesocosms, NO_3^- consumption differed
337 significantly among all velocity treatments, and was enhanced on average by a factor of 5 passing
338 from the stagnant condition to the 6 cm s^{-1} velocity (Table 2; Fig. 2a). In bare sediments, NO_3^-
339 removal rates were not significantly different among velocity treatments. The interaction between
340 light condition and velocity level was not significant for both vegetated and bare sediments (Table
341 2).

342

343 *3.2 Denitrification rates*

344 Dissolved N_2 concentrations measured at the beginning of the incubations were in the range
345 470-525 µM. These values were higher than the theoretical equilibrium values in all sampling
346 events, corresponding to a constant oversaturation in the range 100-104% (pooled data). Consistent
347 with the NO_3^- decline, an increase of N_2 concentrations was detected over the incubation time in all
348 treatments. N_2 concentrations measured at the end of incubations always exceeded those predicted
349 by only gas re-equilibration with the atmosphere, thus the excess was ascribed to internal N_2
350 production.

351 Considering the whole k600 range for each velocity level, average N_2 production rates varied
352 between 838±462 (stagnant condition, light) and 10053±1844 µmol N m^{-2} h^{-1} (6 cm s^{-1}, dark) in
353 vegetated sediments, and between 558±534 (stagnant condition, light) and 1798±363 µmol N m^{-2} h^{-1}
354 (6 cm s^{-1}, dark) in bare sediments (Table 3; Fig. 2b). Denitrification rates were higher in vegetated

mesocosms compared to bare sediments and higher in dark than in light conditions (Table 3; Table 3; Fig. 2b). Denitrification differed significantly among all velocity treatments in vegetated mesocosms, and it was enhanced on average by a factor of 6 and 11 for dark and light, respectively, when passing from the stagnant condition to the 6 cm s^{-1} velocity (Table 2; Fig. 2b). In bare sediments denitrification rates were not significantly different among velocity treatments, similarly to NO_3^- removal rates (Table 2; Fig. 2b).

3.3 N fluxes across the velocity range: NO_3^- removal, N_2 production and plant N uptake

Daily NO_3^- removal rates ranged between 30 and 150 mmol N m^{-2} d^{-1} in vegetated sediments and between 14 and 19 mmol N m^{-2} d^{-1} in bare sediments (Fig. 3). The difference between NO_3^- removal measured in vegetated and bare sediments was minimum in stagnant water. The NO_3^- removal rates detected in vegetated sediments were almost double compared to bare sediments for stagnant conditions while they became more than ten times larger, respectively, when the 6 cm s^{-1} velocity was applied. Daily NO_3^- consumption increased substantially from 0 to 1.5 cm s^{-1} velocity (+257%), while the raise was slight when velocity passed from 1.5 to 3 cm s^{-1} (+15%), and from 3 to 6 cm s^{-1} (+22%). N accumulation in new plant tissues averaged 6±2 mmol N m^{-2} d^{-1}, accounting for 3.1-6-8% of the daily NO_3^- removal.

Considering the whole k600 range for each velocity level, average daily N_2 production rates varied across the velocity range between 27 and 233 mmol N m^{-2} d^{-1} in vegetated sediments and between 18 and 33 mmol N m^{-2} d^{-1} in bare sediments (Fig. 3). Daily rates of denitrification in vegetated sediments increased linearly with increasing water velocity from 0 to 6 cm s^{-1} (Fig. 4). The difference between N_2 flux measured in vegetated and bare sediments was minimum in stagnant water (1.5-fold higher in presence of *P. australis*) and increased together with velocity, reaching the maximum at 6 cm s^{-1} condition (9-fold higher in presence of *P. australis*). Daily rates of NO_3^- removal and denitrification in vegetated sediments were significantly correlated ($r=0.87$, $p<0.001$, $n=24$) (Fig. 5).

4. Discussion

4.1. Water velocity as driver of N removal in vegetated canals

NO_3^- removal via denitrification was strongly affected by flow conditions, despite the narrow range of velocities employed to simulate those conditions commonly found in ditches and canals of lowland agricultural watersheds. A variation of velocity from null to 6 cm s^{-1} produced a rise of one order of magnitude in NO_3^- removal and denitrification rates in vegetated sediments. It is known that overlying velocity conditions control the fluxes of solutes to the bioactive uptake surfaces (Silvester and Sleigh, 1985; Carleton and Mohamoud, 2013). The stimulating effect of velocity on denitrification has been ascribed to the continuous mixing of NO_3^--poor water layers around microbially active surfaces with the overlying NO_3^--rich water, which ensures a constant supply of NO_3^- to the benthic microbial community. The results of the study can verify the observations of Larned et al. (2004) and Arnon et al. (2007a) that increased water flow reduces the thickness of the diffusive boundary layer, eliminates the mass transfer limitations, and enhances the transport of NO_3^- deeper into sediments and biofilms, preventing that the rate of consumption is faster that the rate of delivery.

Previous laboratory experiments (Arnon et al., 2007a; O'Connor and Hondzo, 2007) made for analysing the effects of flow velocity on NO_3^- consumption in benthic biofilms, revealed that the complex interplay between the NO_3^- transport to anoxic niches and the redox state of the benthic compartment mediated by water movement, regulates NO_3^- dissipation via denitrification. A significant decrease of denitrification was observed when flow velocity increased above a specific threshold due to the inhibitory effect of higher oxygen delivery. In fact, most denitrifiers are facultative anaerobes and they shift to aerobic metabolism when oxygen is available, thus the process is suppressed when benthic and epiphytic biofilms are more oxygenated in a higher flow (Arnon et al., 2007b). In our experiment, daily rates of denitrification increased linearly with increasing water velocity with the highest rates measured at the fastest velocity (Fig. 4). This

suggests that the threshold where denitrification is suppressed by high oxygen concentrations was not reached within the range of employed velocities. Based on these results, it can be assumed that increasing velocity likely increased the delivery of oxygen to biofilms concurrently stimulating oxygen consumption by other processes like respiration and oxidation of reduced compounds maintaining favourable conditions for denitrification. An increase of oxygen consumption by the macrophyte-periphyton complex in relation to water movement was previously observed (Dawson et al., 1981; Eriksson, 2001).

Denitrification rates measured in control stagnant conditions were probably regulated by the high respiration rates of sediment, vegetation and associated epiphytes which reduced oxygen concentration promoting denitrification (Eriksson, 2001). However, the measured rates are probably higher compared to natural conditions due to the short term (few hours) of the incubations, and by the addition of NO_3^- at the zero time. In natural, permanently stagnant waters, NO_3^- transport and supply is expected to be much lower. This condition will eventually impede denitrification to occur, even if there is an anoxic environment suitable for the process (Seitzinger et al., 2006).

The positive correlation between denitrification and NO_3^- consumption rates measured at all flow velocity levels in vegetated sediments suggests that denitrification was the main process responsible for NO_3^- dissipation in water column (Fig. 5). However, N_2 flux quantification suffers from the variability introduced by the conservative approach of using a set of empirical depth–velocity equations providing a range of k600 values. Therefore, when the obtained N_2 fluxes were on average greater than the corresponding NO_3^- fluxes, as in the case of the highest velocity employed in the experiments, two explanations can be given: 1) overestimation of N_2 fluxes due to overestimation of the gas transfer velocity; 2) contribution of nitrification in producing additional NO_3^-, which was also denitrified to N_2. Extensive literature reviews have highlighted that empirically derived formulas predicting the gas transfer velocity only as a function of hydraulic parameters (i.e. water velocity and depth) generally tend to overestimate k600 values (Cox et al., 2003), thus it cannot be excluded a consequent overestimation of denitrification rates. Future

applications of the N_2 open-channel method, both at field or laboratory scale, should include the simultaneous direct measurement of reaeration coefficients in order to increase the accuracy of denitrification estimates. Nitrification-denitrification coupling could also have contributed in the difference between NO_3^- consumption and N_2 production. We cannot exclude that part of the N_2 fluxes was also supported by nitrification of mineralized ammonium occurring in biofilms of the sediment or on submerged plant stems (Eriksson and Weisner, 1999).

4.2 Emergent vegetation as a key factor controlling NO_3^- removal via denitrification

NO_3^- removal rates detected in vegetated mesocosms across the velocity range were found to be from 2 to 12-times higher than in bare sediments. Vegetation enhances NO_3^- abatement from polluted water bodies through two main pathways, nutrient uptake and microbial denitrification. Rooted macrophytes stimulate denitrification directly by the exudation of organic carbon from roots, i.e. the energy source for the heterotrophic NO_3^- reduction, and indirectly, by providing surfaces for the growth of epiphytic biofilms where a number of metabolic processes, among which nitrification and denitrification, can occur (Eriksson and Weisner, 1999; Toet et al., 2003; Srivastava et al., 2016). Moreover, oxygen injection into the rhizosphere via aerenchyma creates a mosaic of oxic and anoxic niches, where microbial processes requiring contrasting redox condition can simultaneously occur, as coupled nitrification–denitrification (Kreiling et al., 2011; Gagnon et al., 2012; Paranychianakis et al., 2016). Indeed, a visual check across the transparent mesocosm walls revealed that *P. australis* roots were surrounded by light brown halos, indicating oxidized conditions, while in bare sediments dark brown-blackish zones were observed indicating anoxic conditions. The dense development of periphyton on submersed plant shoots was on average 2.4 times (range 1.6-2.8) larger from the area of bare sediment. This could also be considered an additional factor of increased denitrification without taking into account the direct plant effects on N metabolism. Active denitrification in periphyton on shoots of *P. australis* has been previously demonstrated in eutrophic ecosystems (Toet et al., 2003; Venterink et al., 2003).

459 N_2 production was systematically higher in dark than in light conditions, as expected from
460 diurnal patterns of variation in denitrification rates (Harrison et al., 2005). During light conditions,
461 benthic microalgal photosynthesis and oxygen transport towards the rhizosphere, mediated by *P.*
462 *australis* aerenchyma, enhance the volume of the oxic sediment layer. It also displaces the
463 denitrification zone deeper from the sediment-water interface increasing the diffusional path length
464 of NO_3^- and inhibiting its consumption via denitrification. Similarly, denitrification in biofilms is
465 promoted by elevated oxygen consumption and it is inhibited by photosynthesis of the periphyton
466 algal component. Conversely, in dark conditions, the absence of O_2 production results in a thinner
467 diffusional path length of NO_3^- across the oxic layers enhancing its supply to denitrifiers (Toet et
468 al.; 2003; Nizzoli et al., 2014).
469 A decrease in water column NO_3^- concentrations can also be attributed to assimilation by
470 bacteria, phytoplanktonic and benthic microalgae and reeds and this would explain the difference
471 between NO_3^- removal and the correspondent N_2 production. However, the experimental activities
472 were performed under typical midsummer conditions, when biomass production had almost
473 completed, plant growth was at minimum and N uptake was limited to the maintenance of basic
474 metabolism. Thus, N uptake by *P. australis* accounted for a minor fraction of NO_3^- consumption,
475 less than 5 %, as previously demonstrated (Pierobon et al., 2013; Castaldelli et al., 2015). Uptake by
476 periphyton was not measured but it was expected to have insignificant contribution (Kreiling et al.,
477 2011).
478
479 *4.3 Implications for NO_3^- mitigation in agricultural landscapes*
480 The present outcomes may have relevant applications for the mitigation of excessive NO_3^- in
481 agricultural watersheds by means of phytodepuration in canals networks and wetlands. Considering
482 the increase of denitrification rates due to the increase of flow velocities, it is possible to address a
483 more efficient N removal when designing, restoring and managing aquatic ecosystems. Although N
484 removal is usually a primary goal of natural and constructed wetlands, thematic literature does not

485 report any systematic study dealing with water velocity as a key factor in the regulation of
486 biogeochemical processes and especially denitrification. Field evidences not further adequately
487 investigated demonstrated a greater N removal performance of constructed wetlands in well-mixed
488 compared to stagnant conditions (Sirivedhin and Gray, 2006; Kjellin et al., 2007). Traditionally,
489 wetlands research has focused on hydraulic retention time (i.e. time of contact between water and
490 sediment) and total wet area as key parameters to enhance N removal (Verhoeven et al., 2006;
491 Tournebize et al., in press; Xu et al., 2016). However, in wetlands, water movement is generally
492 negligible and thus diffusive mass transfer limits the supply of NO_3^- from the water column to the
493 denitrification zones. This means that the most of the area of a wetland may not be efficient enough
494 to support high denitrification rates while denitrification may occur only in the portions where a
495 significant flow is maintained. Water velocity enhances NO_3^- availability at all spatial levels, from
496 sediment to the periphytic layers, by favouring the mixing of NO_3^- poor and NO_3^- -rich water in
497 proximity of the microbially active surfaces. From a practical point of view, this means that in a
498 given environment with a certain NO_3^- availability, the artificial regulation of water velocity would
499 allow to maximise the N removal capacity. Furthermore, predictive estimates of depuration
500 potential for NO_3^- can be performed on the base of water velocity, which can be used as key
501 parameter in the decision making for interventions related to river renaturalization or reshaping of a
502 canal section.
503
504 **5. Conclusions**
505 The present study highlighted that hydrodynamic transport conditions may play a key role in
506 regulating N dissipation in slow-flow shallow waterways, by affecting the supply of NO_3^- from the
507 water column to the anoxic niches where denitrification occurs. In particular: 1) sediments
508 colonised by emergent vegetation were found more efficient than bare sediments in removing NO_3^-
509 via denitrification; 2) denitrification in vegetated sediments was the dominant N removal pathway;
510 3) denitrification rates were positively correlated to flow velocity in vegetated sediments indicating

one order of magnitude larger values over a narrow range of velocity increase (from 0 to 6 cm s^{-1}). This study provides the first description of the functional relationship between water velocity and denitrification in slow-flow watercourses and can be used in reclamation works to maximize N-buffer capacity of drainage networks in agricultural landscapes.

Acknowledgments

This work was financially supported by the Emilia-Romagna Region within the Rural Development Programme (PSR) 2014-2020 and within the POR FESR 2007-2013 Programme for the development of the regional High Technology Network. It was also supported by the Po Delta Regional Park of the Emilia-Romagna within a long-term research collaboration for the definition of management protocols for the control of eutrophication in the Po River delta.

References

Allen, R. G., Pereira, L. S., Raes, D., Smith, M. (1998). Crop evapotranspiration-Guidelines for computing crop water requirements-FAO Irrigation and drainage paper 56. FAO, Rome, 300(9), D05109.

Arheimer, B., Pers, B.C., 2016. Lessons learned? Effects of nutrient reductions from constructing wetlands in 1996–2006 across Sweden. Ecol. Eng. In press.

Armstrong, F.A.J., Sterus, C.R., Strickland, J.D.H., 1967. The measurement of upwelling and subsequent biological processes by means of the Technicon AutoAnalyzer and associated equipment. Deep-Sea Res. 14, 381–389.

Arnon, S., Gray, K.A., Packman, A.I., 2007a. Biophysicochemical process coupling controls nitrogen use by benthic biofilms. Limnol. Oceanogr. 52(4), 1665–1671.

534 Arnon, S., Peterson, C. G., Gray, K. A., Packman, A. I., 2007b. Influence of flow conditions and
535 system geometry on nitrate use by benthic biofilms: implications for nutrient mitigation. Environ.
536 Sci. Technol. 41(23), 8142–8148.

537 Arnon, S., Yanuka, K., Nejidat, A., 2013. Impact of overlying water velocity on ammonium uptake
538 by benthic biofilms. Hydrol. Process. 27(4), 570–578.

539 Bartoli, M., Racchetti, E., Delconte, C.A., Sacchi, E., Soana, E., Laini, A., Longhi, D., Viaroli, P.,
540 2012. Nitrogen balance and fate in a heavily impacted watershed (Oglio River, Northern Italy): in
541 quest of the missing sources and sinks. Biogeosciences 9(1), 361–373.

542 Baulch, H.M., Venkiteswaran, J.J., Dillon, P.J., Marange, R., 2010. Revisiting the application of
543 open-channel estimates of denitrification. Limnol. Oceanogr-Meth. 8, 202–215.

544 Biggs, J., von Fumetti, S., Kelly-Quinn, M., 2017. The importance of small waterbodies for
545 biodiversity and ecosystem services: implications for policy makers. Hydrobiologia 793(1), 3–39.

546 Carleton, J.N., Mohamoud, Y.M., 2013. Effect of flow depth and velocity on nitrate loss rates in
547 natural channels. J Am. Water Resour. As. 205–216.

548 Castaldelli, G., Soana, E., Racchetti, E., Vincenzi, F., Fano, E. A., Bartoli, M., 2015. Vegetated
549 canals mitigate nitrogen surplus in agricultural watersheds. Agr. Ecosyst. Environ. 212, 253–262.

550 Cole, J.J., Caraco, N.F., 1998. Atmospheric exchange of carbon dioxide in a low wind oligotrophic
551 lake measured by the addition of SF6. Limnol. Oceanogr. 43, 647–656.

552 Cox, B.A., 2003. A review of dissolved oxygen modelling techniques for lowland rivers. Sci. Total
553 Environ. 314, 303–334.

554 Dalsgaard, T., Nielsen, L.P., Brotas, V., Viaroli, P., Underwood, G.J.C., Nedwell, D.B., Sundbäck,
555 K., Rysgaard, S., Miles, A., Bartoli, M., Dong, L., Thornton, D.C.O., Ottosen, L.D.M., Castaldelli,
556 G., Risgaard-Petersen, N., 2000. Protocol Handbook for NICE-Nitrogen Cycling in Estuaries: A

557 Project Under the EU Research Programme. Marine Science and Technology (MAST III). National
558 Environmental Research Institute, Silkeborg, Denmark, 62 pp

559 Dawson, F.H., Westlake, D.F., Williams, G.I., 1981. An automatic system to study the responses of
560 respiration and photosynthesis by submerged macrophytes to environmental variables.
561 Hydrobiologia 77(3), 277–285.

562 Dollinger, J., Dagès, C., Bailly, J. S., Lagacherie, P., Voltz, M., 2015. Managing ditches for
563 agroecological engineering of landscape. A review. Agron. Sustain. Dev. 35(3), 999–1020.

564 Eloubaldy, A.F., 1969. Wind waves and the reaeration coefficient in open channel flow. Ph.D.
565 Thesis, Colorado State University. Fort Collins, Colorado.

566 Eriksson, P.G., Weisner, S.E.B., 1999. An experimental study on effects of submersed macrophytes
567 on nitrification and denitrification in ammonium-rich aquatic systems. Limnol. Oceanogr. 44(8),
568 1993–1999.

569 Eriksson, P.G., 2001. Interaction effects of flow velocity and oxygen metabolism on nitrification
570 and denitrification in biofilms on submersed macrophytes. Biogeochemistry 55(1), 29–44.

571 Gagnon, V., Chazarenc, F., Kõiv, M., Brisson, J., 2012. Effect of plant species on water quality at
572 the outlet of a sludge treatment wetland. Water Res. 46(16), 5305–5315.

573 Garnier J., Billen G., Vilain G., Benoit M., Passy P., Tallec G., Tournebize J., Anglade J., Billy C.,
574 Mercier B., Ansart P., Azougui A., Sebilo M., Kao C. 2014. Curative vs. preventive management of
575 nitrogen transfers in rural areas: Lessons from the case of the Orgeval watershed (Seine River basin,
576 France). J Environ. Manage. 144, 125–134.

577 Genereux D.P., Hemond H.F., 1992. Gas exchange rate constant for a small stream on Walker
578 Branch watershed, Tennessee. Water Resour. Res. 28, 2365–2374.

579 Harrison, J.A., Matson, P.A., Fendorf, S.E., 2005. Effects of a diel oxygen cycle on nitrogen
580 transformations and greenhouse gas emissions in a eutrophied subtropical stream. Aquat. Sci. 67(3),
581 308–315.

582 Ilyas, H., Masih, I., 2017. The performance of the intensified constructed wetlands for organic
583 matter and nitrogen removal: A review. J Environ. Manage. 198, 372–383.

584 Isaacs, W.P., Gaudy, A.F., 1968. Atmospheric oxygenation in a simulated stream. J Sanit. Eng. Div.
585 Asce 94(SA2), 319–314.

586 Isaacs W.P., Chulavachana, P., Bogart, R., 1969. An experimental study of the effect of channel
587 surface roughness on the reaeration rate coefficient. Proceedings of the 24th Industrial Waste
588 Conference, Purdue University. 1464–1476

589 Jacobs, A.E., Harrison, J.A., 2014. Effects of floating vegetation on denitrification, nitrogen
590 retention, and greenhouse gas production in wetland microcosms. Biogeochemistry 119(1-3), 51–
591 66.

592 Jähne, B., Munnich, K.O., Bosinger, R., Dutzi, A., Huber, W., Libner, P., 1987. On parameters
593 influencing air–water exchange. J Geophys. Res. 92, 1937–1949.

594 Kareiva, P., Watts, S., McDonald, R., Boucher, T., 2007. Domesticated nature: shaping landscapes
595 and ecosystems for human welfare. Science 316(5833), 1866–1869.

596 Kjellin, J., Hallin, S., Wörman, A., 2007. Spatial variations in denitrification activity in wetland
597 sediments explained by hydrology and denitrifying community structure. Water Research, 41(20),
598 4710-4720.

599 Kreiling, R. M., Richardson, W. B., Cavanaugh, J. C., & Bartsch, L. A., 2011. Summer nitrate
600 uptake and denitrification in an upper Mississippi River backwater lake: the role of rooted aquatic
601 vegetation. Biogeochemistry, 104(1-3), 309-324.

602 Kröger, R., Scott, J. T., Czarnecki, J.M.P., 2014. Denitrification potential of low-grade weirs and
603 agricultural drainage ditch sediments in the Lower Mississippi Alluvial Valley. Ecol. Eng. 73, 168–
604 175.

605 Larned, S.T., Nikora, V. I., Biggs, B.J., 2004. Mass-transfer-limited nitrogen and phosphorus
606 uptake by stream periphyton: A conceptual model and experimental evidence. Limnol. Oceanogr.
607 49(6), 1992–2000.

608 Laursen A.E., Seitzinger S.P., 2002. Measurement of denitrification in rivers: an integrated, whole
609 reach approach. Hydrobiologia 485 67–81.

610 Leip, A., Billen, G., Garnier, J., Grizzetti, B., Lassaletta, L., Reis, S., Simpson, D., Sutton, M.A., De
611 Vries, W., Weiss, F., Westhoek, H., 2015. Impacts of European livestock production: nitrogen,
612 sulphur, phosphorus and greenhouse gas emissions, land-use, water eutrophication and biodiversity.
613 Environ. Res. Lett. 10(11), 115004.

614 Madsen, T.V., Sand-Jensen, K., 1991. Photosynthetic carbon assimilation in aquatic macrophytes.
615 Aquat. Bot. 41, 5–40.

616 Moore, M.T., Locke, M.A., Kröger, R., 2016. Using aquatic vegetation to remediate nitrate,
617 ammonium, and soluble reactive phosphorus in simulated runoff. Chemosphere 160, 149–154.

618 Negulescu, M, Rojanski V., 1969. Recent research to determine reaeration coefficient. Water Res.
619 3, 189–202.

620 Nikora, V., 2010. Hydrodynamics of aquatic ecosystems: an interface between ecology,
621 biomechanics and environmental fluid mechanics. River Res. Appl. 26(4), 367–384.

622 Nizzoli, D., Welsh, D.T., Longhi, D., Viaroli, P., 2014. Influence of *Potamogeton pectinatus* and
623 microphytobenthos on benthic metabolism, nutrient fluxes and denitrification in a freshwater littoral
624 sediment in an agricultural landscape: N assimilation versus N removal. Hydrobiologia 737, 183–
625 200.

O'Connor, B.L., Hondzo, M., 2007. Enhancement and inhibition of denitrification by fluid-flow and dissolved oxygen flux to stream sediments. Environ. Sci. Technol. 42(1), 119–125.

Padden, T.J., Gloyna, E.F., 1972. Simulation of stream processes in a model river. Technical Report No. 2 (EHE-70-23, CRWR-72). Austin, Texas: Texas University, Center for Reasearch in Water Resources.

Palumbo, J.E., Brown, L.C., 2013. Assessing the performance of reaeration prediction equations. J Environ. Eng. 140(3), 04013013.

Paranychianakis, N.V., Tsiknia, M., Kalogerakis, N., 2016. Pathways regulating the removal of nitrogen in planted and unplanted subsurface flow constructed wetlands. Water Res. 102, 321–329.

Pierobon, E., Castaldelli, G., Mantovani, S., Vincenzi, F., Fano, E.A., 2013. Nitrogen removal in vegetated and unvegetated drainage ditches impacted by diffuse and point sources of pollution. CLEAN Soil Air Water 41, 24–31.

Reisinger, A. J., Tank, J. L., Hoellein, T. J., Hall, R. O., 2016. Sediment, water column, and open-channel denitrification in rivers measured using membrane-inlet mass spectrometry. Journal of Geophysical Research: Biogeosciences, 121(5), 1258–1274.

Revsbech, N.P., Jacobsen, J.P., Nielsen, L.P., 2005. Nitrogen transformations in microenvironments of river beds and riparian zones. Ecol. Eng. 24(5), 447–455.

Romero, E., Garnier, J., Billen, G., Peters, F., Lassaletta, L., 2016. Water management practices exacerbate nitrogen retention in Mediterranean catchments. Sci. Total Environ. 573, 420–432.

Seitzinger, S., Harrison, J.A., Böhlke, J.K., Bouwman, A.F., Lowrance, R., Peterson, B., Tobias, C., Drecht, G.V., 2006. Denitrification across landscapes and waterscapes: a synthesis. Ecol. Appl. 16(6), 2064-2090.

Shen, L.D., Zheng, P. H., Ma, S.J., 2016. Nitrogen loss through anaerobic ammonium oxidation in agricultural drainage ditches. Biol. Fert. Soils 52(2), 127–136.

650 Silvester, N.R., Sleigh, M.A., 1985. The forces on microorganisms at surfaces in flowing
651 water. Freshwater Biol. 15(4), 433–448.

652 Sirivedhin, T., Gray, K.A., 2006. Factors affecting denitrification rates in experimental wetlands:
653 field and laboratory studies. Ecol. Eng. 26(2), 167-181.

654 Srivastava, J.K., Chandra, H., Kalra, S.J., Mishra, P., Khan, H., Yadav, P., 2016. Plant–microbe
655 interaction in aquatic system and their role in the management of water quality: a review. Appl.
656 Water Sci. 1–12.

657 Soana, E., Balestrini, R., Vincenzi, F., Bartoli, M., Castaldelli, G., 2017. Mitigation of nitrogen
658 pollution in vegetated ditches fed by nitrate-rich spring waters. Agr. Ecosyst. Environ. 243, 74–82.

659 Taylor, J.M., Moore, M.T., Scott, J.T., 2015. Contrasting nutrient mitigation and denitrification
660 potential of agricultural drainage environments with different emergent aquatic macrophytes. J.
661 Environ. Qual. 44(4), 1304–1314.

662 Toet, S., Huibers, L.H., Van Logtestijn, R.S., Verhoeven, J.T., 2003. Denitrification in the
663 periphyton associated with plant shoots and in the sediment of a wetland system supplied with
664 sewage treatment plant effluent. Hydrobiologia 501(1-3), 29–44.

665 Törnqvist, R., Jarsjö, J., Thorslund, J., Rao, P. S. C., Basu, N. B., Destouni, G., 2015. Mechanisms
666 of basin-scale nitrogen load reductions under intensified irrigated agriculture. PloS One 10(3):
667 e0120015.

668 Tournebize, J., Chaumont, C., Mander, Ü., 2017. Implications for constructed wetlands to mitigate
669 nitrate and pesticide pollution in agricultural drained watersheds. Ecol. Eng. In press.

670 Valiela, I., Bowen, J.L., 2002. Nitrogen sources to watersheds and estuaries: role of land cover
671 mosaics and losses within watersheds. Environ. Pollut. 118(2), 239–248.

672 Venterink, H.O., Hummelink, E., Van den Hoorn, M.W., 2003. Denitrification potential of a river
673 floodplain during flooding with nitrate-rich water: grasslands versus reedbeds. Biogeochemistry
674 65(2), 233–244.

675 Veraart, A.J., Dimitrov, M.R., Schrier-Uijl, A.P., Smidt, H., de Klein, J.J., 2016. Abundance,
676 activity and community structure of denitrifiers in drainage ditches in relation to sediment
677 characteristics, vegetation and land-use. Ecosystems 1–16.

678 Verhoeven, J.T., Arheimer, B., Yin, C., Hefting, M.M., 2006. Regional and global concerns over
679 wetlands and water quality. Trends Ecol. Evol. 21(2), 96–103.

680 Wanninkhof, R., 1992. Relationship between gas exchange and wind speed over the ocean. J.
681 Geophys. Res. 97, 7373–7381.

682 Weigelhofer, G., Welti, N., Hein, T., 2013. Limitations of stream restoration for nitrogen retention
683 in agricultural headwater streams. Ecol. Eng. 60, 224–234.

684 Weiss, R.F., 1970. The solubility of nitrogen, oxygen and argon in water and seawater. Deep-Sea
685 Res. 17(4), 721–735.

686 Xiong, Y., Peng, S., Luo, Y., Xu, J., Yang, S., 2015. A paddy eco-ditch and wetland system to
687 reduce non-point source pollution from rice-based production system while maintaining water use
688 efficiency. Environ. Sci. Pollut. R. 22(6), 4406–4417.

689 Xu Z, Yang Z, Yin X, Cai Y, Sun T. 2016. Hydrological management for improving nutrient
690 assimilative capacity in plant-dominated wetlands: A modelling approach. J Environ. Manage. 177,
691 84–92.

692 Zhou, S., Borjigin, S., Riya, S., Terada, A., Hosomi, M., 2014. The relationship between anammox
693 and denitrification in the sediment of an inland river. Sci. Total Environ. 490, 1029–1036.

694 **Table 1.** Water column features at the beginning of each incubation of the first and second
695 experiment. Average values±standard deviation of mesocosms with plants and without plants (*n*=6)
696 are reported. Ranges of gas transfer velocity (k600) for each velocity were calculated as described
697 in the Material and Methods section. Minimum k600 values were obtained by applying the equation
698 proposed by Isaacs et al. (1969), while maximum values resulted from the parameterizations by
699 Padden and Gloyna (1972) and Negulescu and Rojanki (1969).

700

Velocity ($cm\ s^{-1}$)	k600 ($cm\ h^{-1}$)	Dark/Light	T (°C)		Oxygen (µM)		NO_3^- (µM)	
			Exp 1	Exp 2	Exp 1	Exp 2	Exp 1	Exp 2
0	0.48	Dark	26.30 (0.00)	23.06 (0.10)	160 (12)	148 (19)	98 (2)	94 (5)
		Light	25.60 (0.15)	23.57 (0.05)	161 (18)	138 (32)	96 (8)	102 (7)
1.5	0.48-0.99	Dark	27.28 (0.12)	22.70 (0.00)	168 (12)	188 (18)	94 (4)	98 (12)
		Light	27.00 (0.00)	22.45 (0.05)	147 (25)	174 (23)	93 (5)	100 (7)
3	0.98-1.63	Dark	26.18 (0.04)	22.53 (0.05)	156 (8)	174 (21)	91 (7)	104 (6)
		Light	24.40 (0.00)	22.73 (0.37)	165 (11)	161 (32)	99 (9)	98 (9)
6	1.95-3.01	Dark	25.97 (0.08)	22.80 (0.00)	157 (14)	183 (26)	96 (11)	96 (7)
		Light	25.80 (0.26)	22.53 (0.37)	166 (10)	183 (27)	92 (7)	101 (7)

701

Table 2. Results of the two–way ANOVA performed to test the effect of factors *velocity* and *light condition (light/dark)* on NO_3^- removal and denitrification rates measured in bare and vegetated mesocosms. Significant differences ($p<0.05$) are reported in bold.

Variable	Factor	df	Sediment + *P. australis* *p*	Sediment *p*
NO_3^- removal	Velocity	3	**<0.001**	0.279
	Light/dark	1	**0.040**	**0.030**
	Velocity x Light/Dark	3	0.137	0.245
Denitrification	Velocity	3	**<0.001**	0.235
	Light/dark	1	**0.012**	**<0.001**
	Velocity x Light/Dark	3	0.568	0.382

706 **Table 3.** Hourly rates of denitrification measured across the velocity range in bare and vegetated
707 mesocosms. Rates obtained in dark and light conditions and by varying the k600 value (minimum,
708 average, and maximum) are compared. Pooled rates from the two experiments are reported
709 (average±standard deviation, *n*=6).

Velocity (cm s^{-1})	Sediment/Sediment+*P. australis*	Dark/Light	Denitrification rate (µmol N m^{-2} h^{-1})		
			k600 min	k600 avg	k600 max
0	Sediment	Dark	-	1116 ± 646	-
	Sediment	Light	-	558 ± 534	-
	Sediment +*P. australis*	Dark	-	1677 ± 882	-
	Sediment +*P. australis*	Light	-	838 ± 462	-
1.5	Sediment	Dark	1368 ± 410	1702 ± 467	2064 ± 522
	Sediment	Light	626 ± 350	775 ± 532	866 ± 619
	Sediment +*P. australis*	Dark	3457 ± 544	4195 ± 612	5048 ± 732
	Sediment +*P. australis*	Light	2406 ± 434	3240 ± 500	4161 ± 616
3	Sediment	Dark	935 ± 591	1048 ± 796	1400 ± 820
	Sediment	Light	571 ± 289	833 ± 438	1191 ± 484
	Sediment +*P. australis*	Dark	4550 ± 486	5844 ± 585	6796 ± 690
	Sediment +*P. australis*	Light	4485 ± 938	5736 ± 1161	6696 ± 1385
6	Sediment	Dark	1506 ± 289	1814 ± 308	2073 ± 327
	Sediment	Light	569 ± 388	783 ± 284	1015 ± 291
	Sediment +*P. australis*	Dark	8166 ± 879	10178 ± 1102	11815 ±1248
	Sediment +*P. australis*	Light	7533 ± 722	9664 ± 823	11337 ± 911

710

Figure captions

Fig. 1. Diagram of annular chambers (a) and incubation system (b).

Fig. 2. Hourly rates of NO_3^- removal (a, average±standard deviation, *n*=6) and denitrification (b, average±standard deviation, *n*=18) measured in bare and vegetated mesocosms across the velocity range. Denitrification rates are reported as average value considering the whole k600 range for each velocity level. For vegetated sediments, differences among velocity treatments are shown on the basis of post-hoc tests ($a<b<c<d$, $p<0.05$). For bare sediments, both NO_3^- removal and denitrification rates were not significantly different among velocity treatments.

Fig. 3. Daily rates of NO_3^- removal (box below, average±standard deviation, *n*=6) and denitrification (box at the top, average±standard deviation, *n*=18) measured in bare and vegetated mesocosms across the velocity range. Denitrification rates are reported as average value considering the whole k600 range for each velocity level.

Fig. 4. Daily denitrification rates in *P. australis* vegetated sediments as a function of water velocity.

Fig. 5. Correlation between daily rates of NO_3^- removal and denitrification in *P. australis* vegetated sediments.

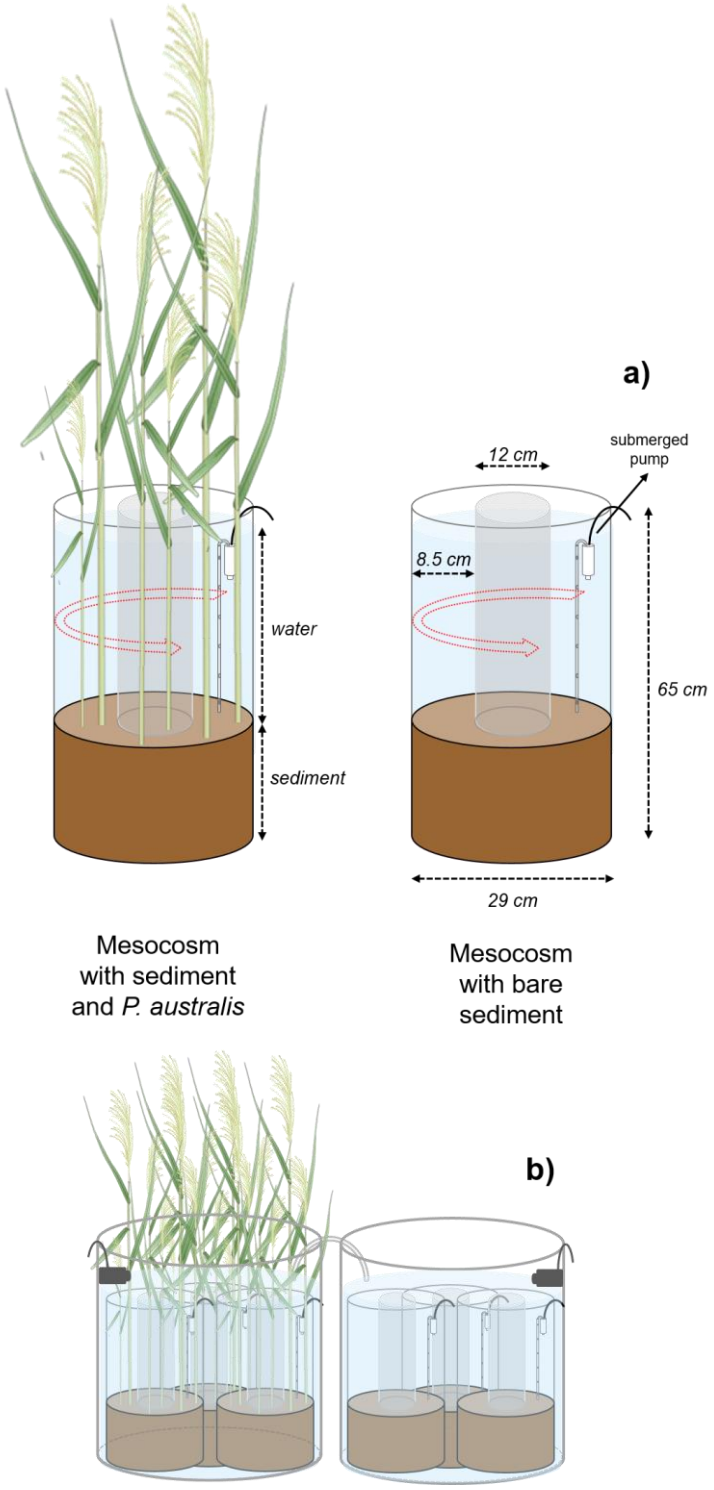
a)
12 cm
submerged
pump
8.5 cm
water
sediment
65 cm
29 cm
Mesocosm
with sediment
and P. australis
Mesocosm
with bare
sediment
b)

727

728 Fig. 1

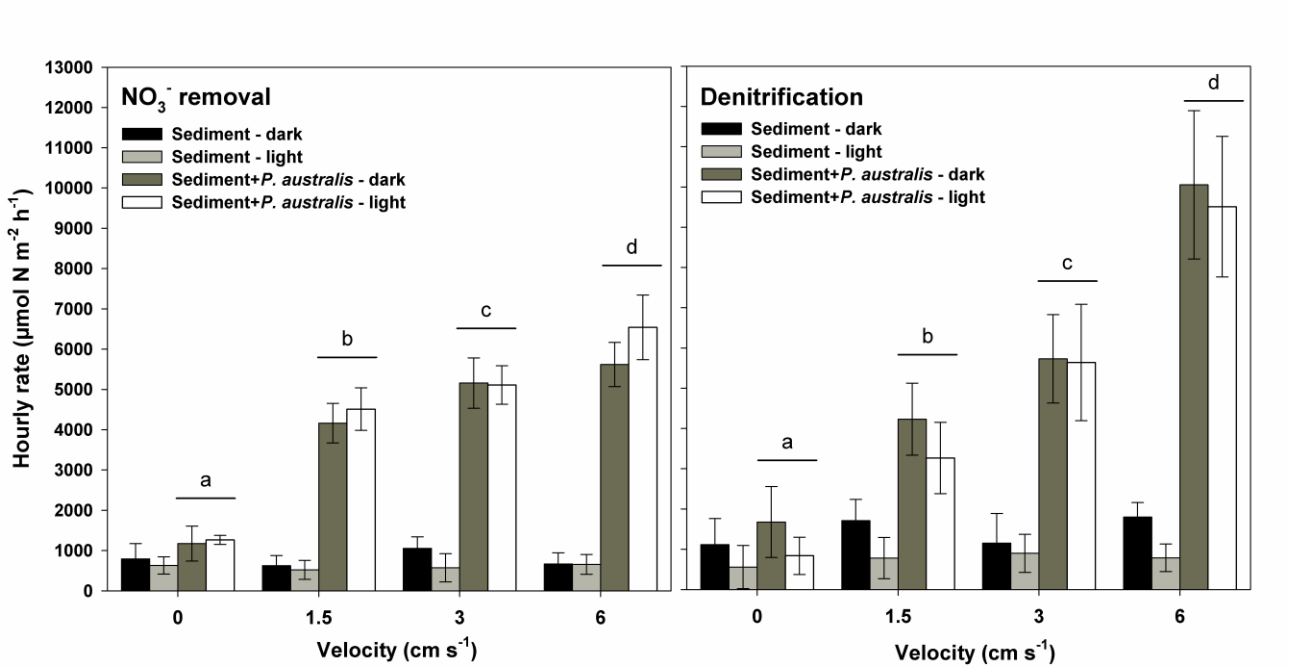
NO3- removal
Denitrification
Sediment - dark
Sediment - light
Sediment+P. australis - dark
Sediment+P. australis - light
Hourly rate (µmol N m-2 h-1)
Velocity (cm s-1)
0
1.5
3
6
a
b
c
d

729

730 Fig. 2

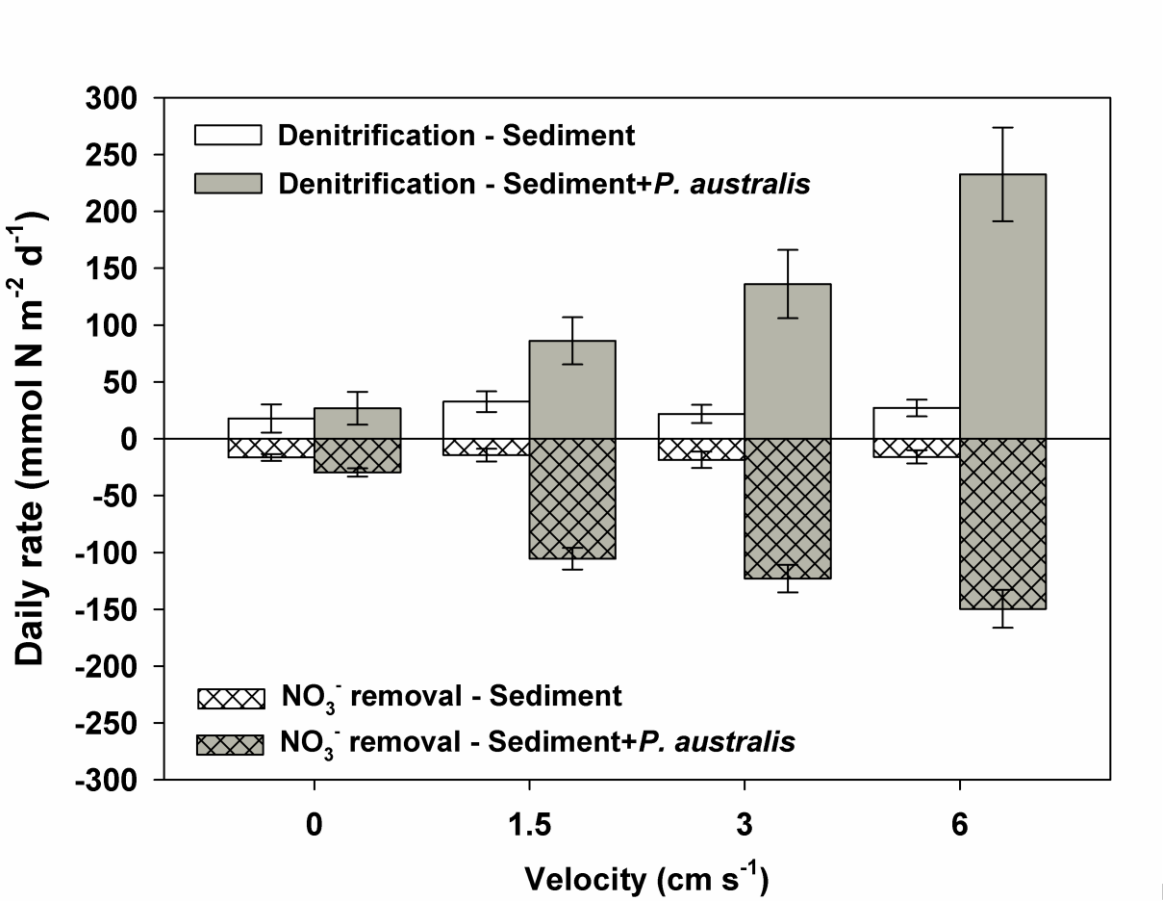
Denitrification - Sediment
Denitrification - Sediment+P. australis
NO3- removal - Sediment
NO3- removal - Sediment+P. australis
Daily rate (mmol N m-2 d-1)
Velocity (cm s-1)
300
250
200
150
100
50
0
-50
-100
-150
-200
-250
-300
0
1.5
3
6

731 Fig. 3

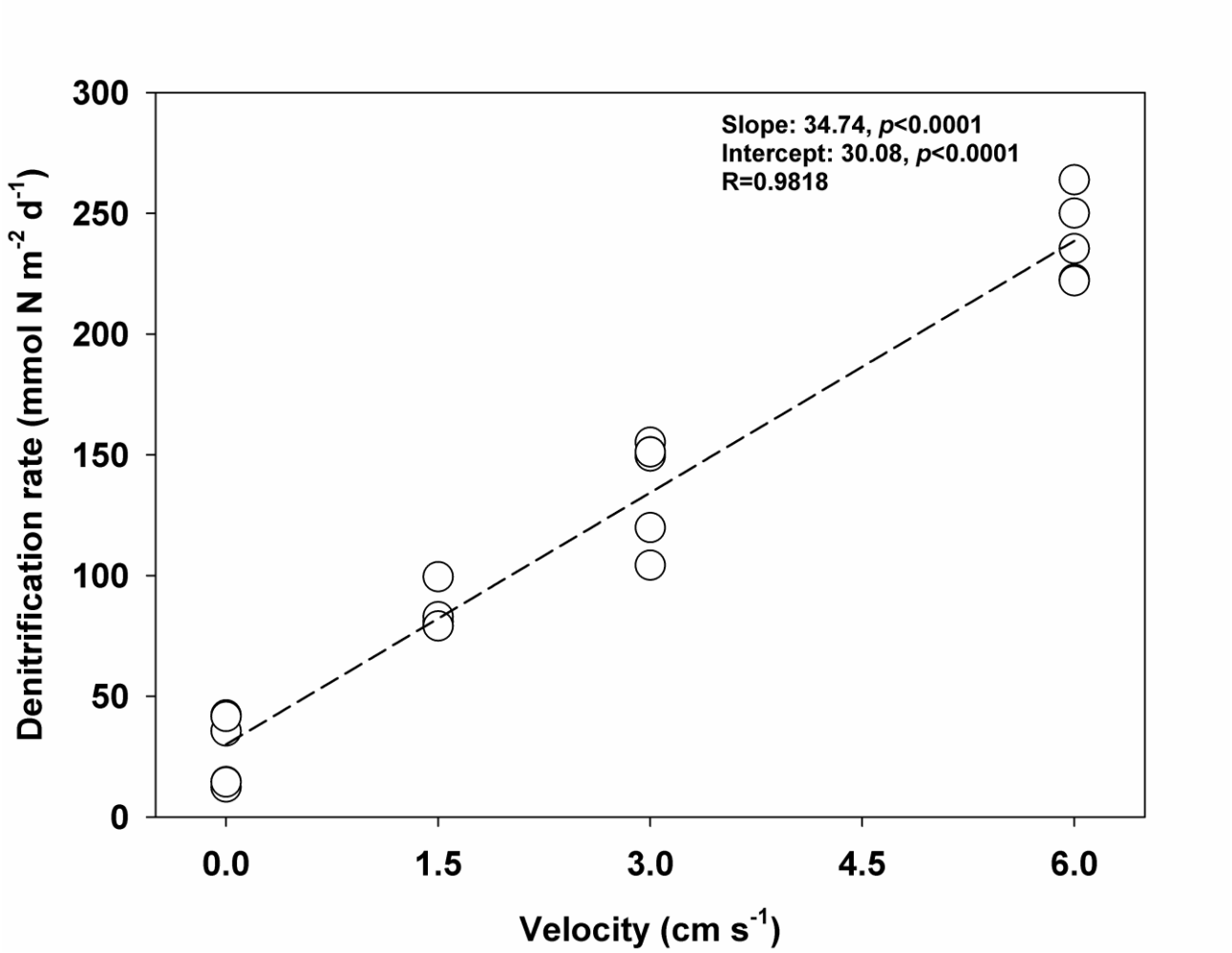
Slope: 34.74, p<0.0001
Intercept: 30.08, p<0.0001
R=0.9818
Denitrification rate (mmol N m-2 d-1)
Velocity (cm s-1)
0
50
100
150
200
250
300
0.0
1.5
3.0
4.5
6.0

732

733 Fig. 4

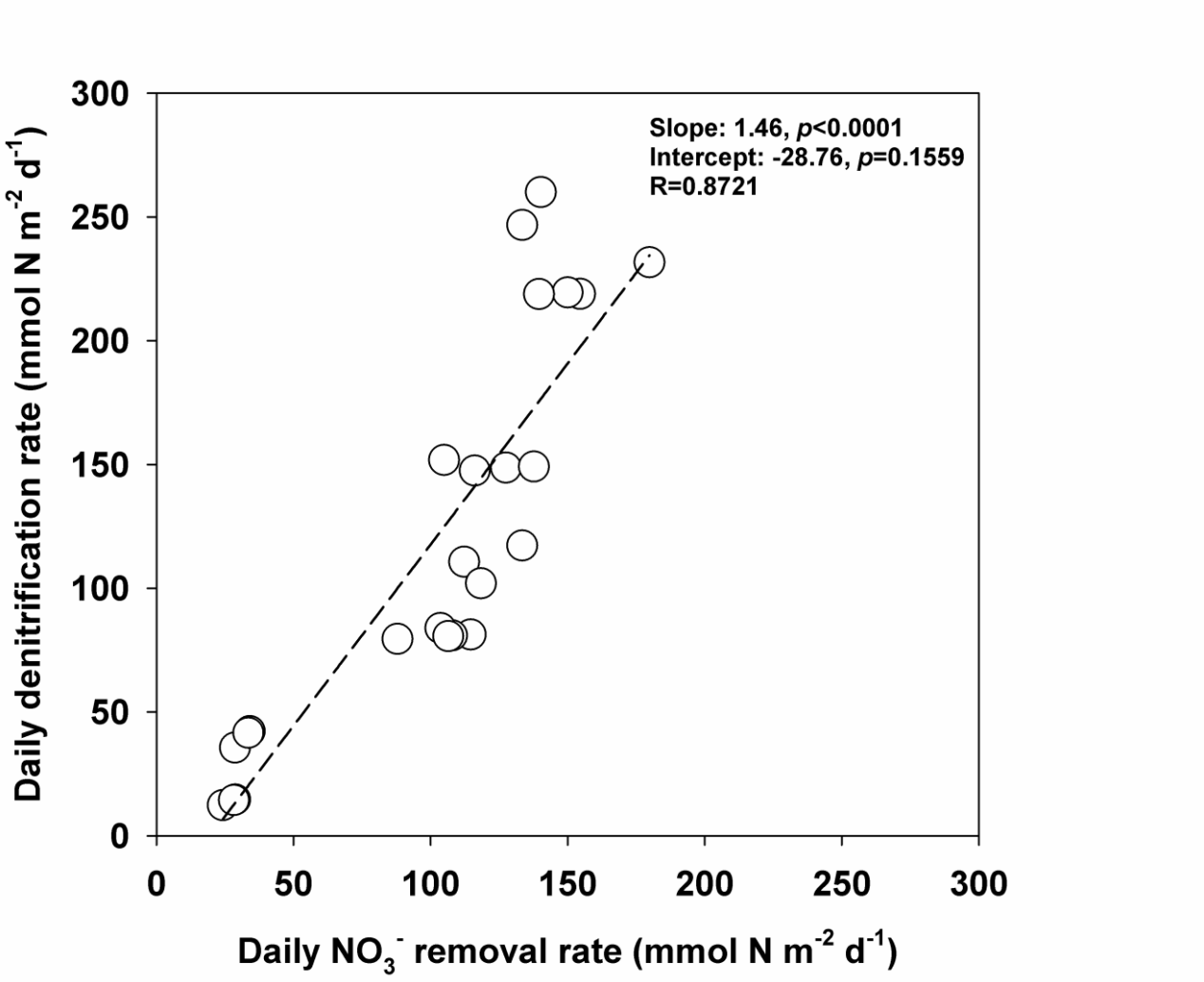
Slope: 1.46, p<0.0001
Intercept: -28.76, p=0.1559
R=0.8721
Daily denitrification rate (mmol N m-2 d-1)
Daily NO3- removal rate (mmol N m-2 d-1)
0
50
100
150
200
250
300

734

735 Fig. 5